Development of a kidney-on-a-chip model for compound screening and transport studies

Vormann, M.K.

Chapter 2

Nephrotoxicity and Kidney Transport Assessment on 3D Perfused Proximal Tubules

MK Vormann, L Gijzen, S Hutter, L Boot, A Nicolas, A van den Heuvel, J Vriend, CP Ng, TTG Nieskens, V van Duinen, B de Wagenaar, R Masereeuw, L Suter-Dick, SJ Trietsch, M Wilmer, J Joore, P Vulto, HL Lanz

Based on:

The AAPS Journal 20, 90. (2018)

Abstract

Proximal tubules in the kidney play a crucial role in reabsorbing and eliminating substrates from the body into the urine, leading to high local concentrations of xenobiotics. This makes the proximal tubule a major target for drug toxicity that needs to be evaluated during the drug development process. Here, we describe an advanced *in vitro* model consisting of fully polarized renal proximal tubular epithelial cells cultured in a microfluidic system. Up to forty leak-tight tubules were cultured on this platform, that provides access to the basolateral as well as the apical side of the epithelial cells. Exposure to the nephrotoxicant cisplatin caused a dose-dependent disruption of the epithelial barrier, a decrease in viability, an increase in effluent LDH activity, and changes in expression of tight-junction marker zona-occludence 1, actin and DNA-damage marker H2A.X, as detected by immunostaining. Activity and inhibition of the efflux pumps P-glycoprotein (P-gp) and multidrug resistance protein (MRP) were demonstrated using fluorescence-based transporter assays. In addition, the transepithelial transport function from the basolateral to the apical side of the proximal tubule was studied. The apparent permeability of the fluorescent P-gp substrate rhodamine 123 was decreased by 35% by co-incubation with cyclosporin A. Furthermore, the activity of the glucose transporter SGLT2 was demonstrated using the fluorescent glucose analog 6-NBDG which was sensitive to inhibition by phlorizin. Our results demonstrate that we developed a functional 3D perfused proximal tubule model with advanced renal epithelial characteristics that can be used for drug screening studies.

Introduction

Renal proximal tubules play a crucial role in reabsorbing salt, water, and organic solutes such as glucose from the glomerular filtrate as well as eliminating endogenous and exogenous waste products from the body [1]. The transepithelial transport of substrates and the concentration of xenobiotics in the tubular lumen make the proximal tubule a target for drug-induced toxicity [2].

Currently, preclinical assessment of nephrotoxicity is mainly performed in animal studies. However, due to ethical concerns and the limited translatability of these models to the human situation, *in vitro* modelling is rapidly becoming important for studying solute transport, drug-induced toxicity and disease-related kidney failure [3]. Current-day *in vitro* models typically comprise human renal proximal tubule cells (RPTECs) grown on a permeable membrane support. But, these systems often lack elements such as flow or embedding in an extracellular matrix (ECM) structure and are not compatible with image-based readouts. Moreover, the permeable support membrane is a crucial barrier influencing both transport parameters and physiology of cells.

In recent years, the use of microfluidics has gained significant interest for building human tissue models of enhanced physiological relevance. These techniques, popularly referred to as Organ-on-a-Chip, add flow to cell culture systems, enable gradient formation, facilitate a 3D architecture

of tissues, allow engineering of tissue complexity through layered co-cultures, and are typically compatible with ECM-embedded cultures. Various model systems for the renal proximal tubule have been reported over the past few years [4]–[7]. Although they represent powerful examples of the added value of microfluidics to the realm of *in vitro* kidney modelling, these chips are largely prototypes, yield single data points per chip, require external tube and pump connections for each chip and are typically constructed of materials that absorb hydrophobic compounds [8].

The current challenge is to implement these prototypes into platforms combined with protocols and assays for routine use in an end-user environment [9], [10]. Robust cell culture protocols are needed that can be performed in parallel in order to test dilution series, including several replicates and appropriate controls. Furthermore, the platform needs to be compatible with a range of assays that are typically used in an *in vitro* environment, including fluorescence-based methods, immunohistochemical staining, barrier integrity monitoring, transport studies, viability assays, qRT-PCR, ELISA's and many others. Last but not least, operation of the platform should straightforward to the level that expert microfluidic skills are not required for end-users. Therefore, the organ-on-a-chip platform needs to be compatible with standard lab equipment such as pipets, (confocal) microscopes, plate readers, and other microwell-plate compatible equipment.

In this research, we used the OrganoPlate [11], a microtiter-plate based microfluidic chip platform enabling forty tissues per plate. A proximal tubule-on-a-chip was modeled with renal proximal tubule epithelial cells [12] (RPTEC, SAK 7 clone) grown as perfused tubules against an ECM.

The cells used for this study were developed and characterized by Li et al [12] and showed similar expression levels of several uptake and efflux transporters when compared to human primary proximal tubule cells. The RPTEC line further showed improved uptake and efflux compared to the HK-2 cell line, with a more sensitive detection of nephrotoxicants. Two of the efflux transporters, P-glycoprotein (P-gp) and multidrug resistance-associated protein 4 (MRP4), showed high levels of expression. Furthermore, the morphology of cell monolayers showed a typical cobblestone structure which is important for tight barriers.

After optimization of growth conditions of RPTEC in the OrganoPlate, tubules were analyzed for polarization of the epithelial layer by immunostaining, and barrier integrity through a live fluorescent dye assay. Next, the platform was evaluated for its suitability in studying (trans-epithelial) transport and drug-induced toxicity. The technology can be implemented in every basic cell laboratory with standard laboratory equipment and can be assessed with multiplexed readouts.

Materials and methods

Cell culture

Renal proximal tubule epithelial cells (RPTEC, Kidney PTEC Control Cells, SA7K Clone, Sigma, Germany, MTOX1030) were cultured on PureCol-coated (Advanced BioMetrix, 5005-B, diluted with 1:30 in HBSS (Sigma H6648), 20 min incubation at 37 °C) T75 flasks in MEME alpha Modification (Sigma, M4526) supplemented with RPTEC Complete Supplement (Sigma, MTOXRCSUP), L-glutamine (1.87 mM, Sigma, G7513), Gentamicin (28 µg/ml, Sigma, G1397) and Amphotericin B (14 ng/ml, Sigma, A2942). Cells were incubated in a humidified incubator (37 °, 5 % CO_2), and every 2-3 days, medium was changed. At 90-100 % confluency, cells were washed with HBSS (Sigma, H6648), detached with accutase (Sigma, A6964), pelleted (140 g, 5 minutes), and used for seeding in the OrganoPlate. Cells for experiments were used up to passage 3.

OrganoPlate culture

For all experiments a three-lane OrganoPlate (Mimetas BV, 4003 400B) with a channel width of 400 µm and a height of 220 µm was used. 1.6 µL of extracellular matrix (ECM) gel composed of 4 mg/ml collagen 1 (AMSbio Cultrex 3D Collagen I Rat Tail, Cat. 3447-319 020-01), 100 mM HEPES (Life Technologies, 15630) and 3.7 mg/mL $NaHCO_3$ (Sigma, 320 S5761) was injected into the middle inlet (fig. 1a) of all 40 chips. After a polymerization time of 20 minutes, 20 µL HBSS was added on top of the collagen 1 and the plate was incubated in a humified incubator at 37 °C over night. After polymerization of the ECM, the plate could be also stored in a humified incubator (37 °C) for up to a week. RPTEC were detached and resuspended in medium at a concentration of 10 x 10^6 cells per mL. 2 µL of the cell suspension (20 x 10^3 cells) was injected into each top inlet, followed by an addition of 50 µL medium to the same well. For control chips, 2 µL of medium was injected into the top inlet instead of the cell suspension. Subsequently, the OrganoPlate was placed for 5 hours at an angle of 70 degree into the incubator (37 °C, 5 % CO_2, humidified). After attachment of the cells 50 µL of medium was added to the top outlet, bottom inlet, bottom outlet (fig. 1a), and HBSS on the gel was removed. The OrganoPlate was placed flat in an incubator on an interval rocker platform (+/- 7 degree angle, 8 min interval) enabling a bidirectional flow though the perfusion channels (See fig. 5S). At day 3 antibiotics (gentamycin and amphotericin B) were removed from the medium. Medium was replaced every 2-3 days. 48-hour toxicant exposures were started at day 6, all other experiments were performed at day 7, 8,9, or 10. To show the effect of flow in the system an OrganoPlate was taken off the rocker platform from day 1 to day 4. At day 4 medium was refreshed and the plate was rocked again under same conditions as the control experiments.

Immunohistochemistry

RPTEC tubes were fixed by replacing the medium with 3.7 % formaldehyde (Sigma, 252549) in HBSS (Sigma, 55037C) for 10 minutes. Tubules were washed with washing solution (4 % fetal bovine serum (Gibco, 16140-071) in HBSS) and permeabilized (0.3 % Triton X-100 (Sigma, T8787) in HBSS) for 10 minutes. Next, cells were incubated for 45 minutes in blocking solution (2 % FBS, 2 % bovine serum albumin (BSA) (Sigma, A2153), and 0.1 % Tween 20 (Sigma, P9416) in HBSS).

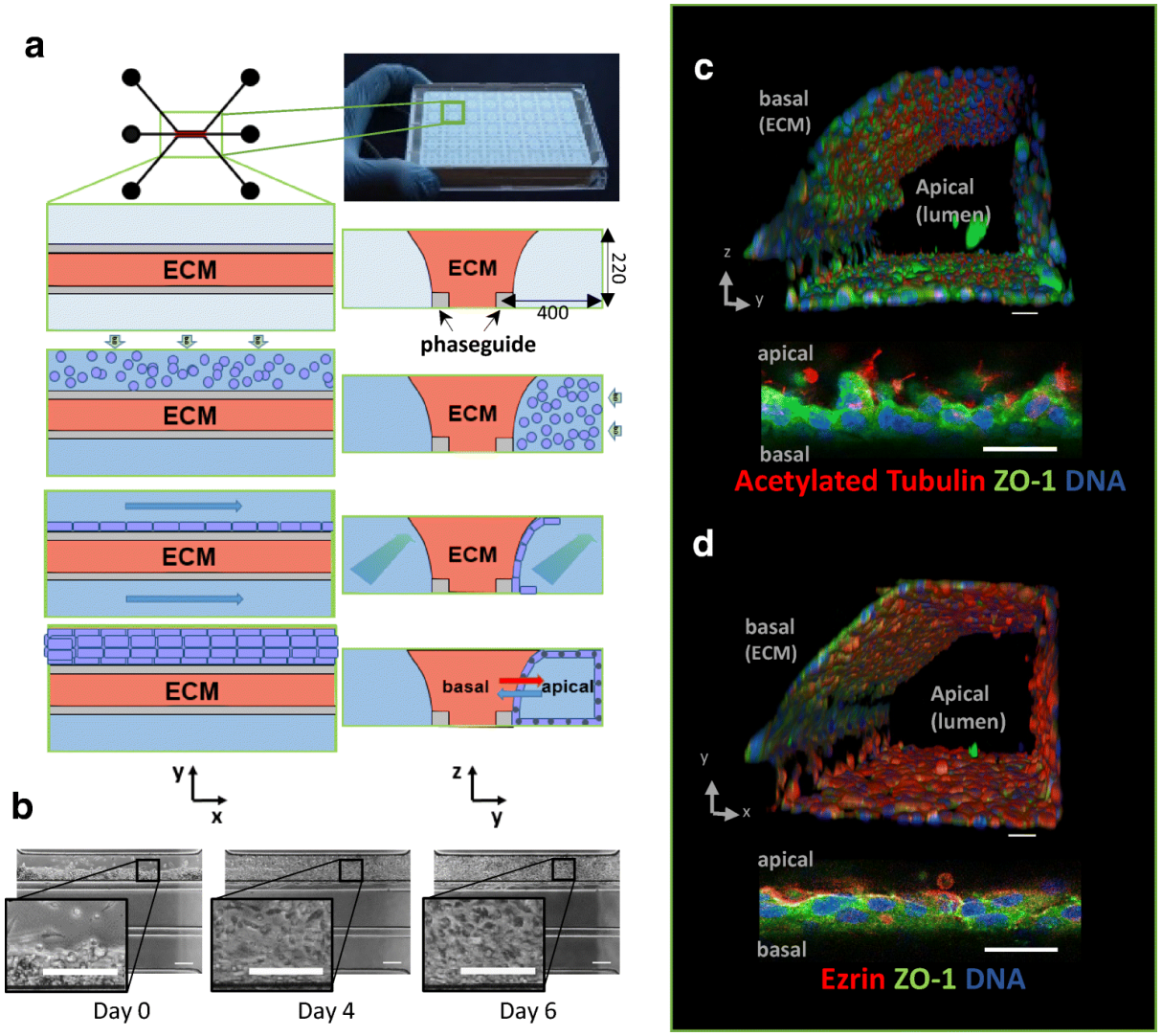

Figure 1: ***Proximal tubule-on-a chip model in the 3-lane OrganoPlate platform. a*** *Seeding RPTEC against collagen 1: After loading collagen 1 into the middle channel cells were seeded in the adjacent channel. By gravity cells are triggered to attach to the gel. After inducing flow RPTEC start growing a perfused tubular structure. Dimensions of the channels are in µm.* ***b*** *Phase contrast images at day 0, day 4, and day 6 after seeding of RPTEC. Images show that RPTEC form a tubular structure in the top channel in 6 days. Scale bar = 200 µm.* ***c,d*** *3D reconstruction images of RPTEC tubules in the OrganoPlate showing a view into the lumen of tubules (apical side). The magnification shows a single z-slice of the cells growing against the ECM. Nuclei in blue. Scale bars = 30 µm.* ***c*** *Image of the tubule showing the presence of cilia (acetylated tubulin, red) pointing into the direction of the lumen. The confluent tubules express ZO-1 at the cell borders which confirms the tight junction formation between neighboring epithelial (green).* ***d*** *Ezrin expression (red) on the apical side and ZO-1 (green) expression at the cell borders of the tubules shows the correct polarization of the cells.*

Hereafter cells were incubated with the primary antibodies, diluted in blocking solution, for 60 minutes at room temperature. Primary antibodies against Ms-a-ezrin (BD Biosciences, 610602, 1:200), Ms-a-acetylated tubulin (Sigma, T6793, 1:4000), Rb-a-Zonula occludens-1 (ZO-1) (Thermo Fischer, 61-7300, 1:125, rabbit), Rb-a-Phospho-Histone (H2A.X) (Cell Signaling Technology, 9718S, 1:200, rabbit), Mouse isotype (Life technologies, 86599), Rabbit isotype (Life technologies, 86199), were used. Subsequently, cells were washed 3 times with washing solution and then incubated for 30 minutes at room temperature with secondary antibodies Gt-a-Ms IgG (H+L) Alexa Fluor 555 (Life Technologies, A21422,1:250), Gt-a-Rb IgG (H+L) Alexa Fluor 488 (Life Technologies, A32731, 1:250) diluted in blocking solution. After washing the tubules three times, nuclei were stained with DraQ5 (Abcam, ab108410, 1:1000) or Nucblue fixed cell stain (Life Technologies, R37606, 2 drops/mL) or Actin red (Life Technologies, R37112, 2 drops/mL) in the last washing step. Fluorescent images for the 3D reconstructions were taken with the Leica SP5-Sted Confocal Microscope. A z-stack of 220 µm with 2 µm between each image plane was imaged with Alexa 488, Alexa 555 and Alexa 647. Fluorescent images for the analysis of the protein expression after a toxicant exposure were taken with the ImageXpress® Micro Confocal High-Content Imaging System (Molecular Devices). A z-stack of 5 µm between each image plane was imaged with for DAPI, FITC, TRITC and Cy5 channels. A maximum projection was created for depicting the images and a summary projection was used for quantifying the fluorescent intensity of the markers.

Barrier integrity assay

The barrier integrity assay (BI assay) was performed by replacing the medium of the perfusion channel with medium containing 0.5 mg/ml TRITC-dextran (4.4 kDa, Sigma, FD20S) and 0.5 mg/ml FITC-dextran (155 kDa, Sigma, T1287). Next, the plate was imaged every two minutes for 12 minutes with the ImageXpress Micro XLS-C High Content Imaging System (Molecular Devices) at 37 °C. Leakage of the dyes from the apical side of the tube to the basal side into the ECM was measured and the ratio between the basal and the apical was analyzed with Fiji [13]. The labeled dextrans can be washed out after each measurement. The permeability of the membranes was analyzed by measuring the amount of molecules which leaked though the membrane into the adjacent gel lane over time. From these measurements the apparent permeability index (P_{app}: initial flux of a compound through a membrane, normalized by membrane surface area and donor concentration) was calculated by the following formula:

$$P_{app} = \frac{\Delta C_{receiver} \times V_{receiver}}{\Delta t \times A_{barrier} \times C_{donor}} \left(\frac{cm}{s}\right)$$

$\Delta C_{receiver}$ is the measured normalized intensity difference of the ECM to the donor channel (fig. 2b) (value of FL_{ECM}/ value of FL_{perf}) at t_{0min} and t_{10min}, $V_{receiver}$ is the volume of the measured region in the ECM channel (fig. 2b, c; channel height x channel with x channel length = 220 µm x 2304 µm x 204.8 µm = 0.0001 cm^2), Δt is the time difference t_{10min}-t_{0min} = 10 minutes, $A_{barrier}$ (0.0057 cm^2

) is the surface of the ECM interface with the medium channel, and C_{donor} is the donor concertation of the dextran dye (0.5 mg/mL).

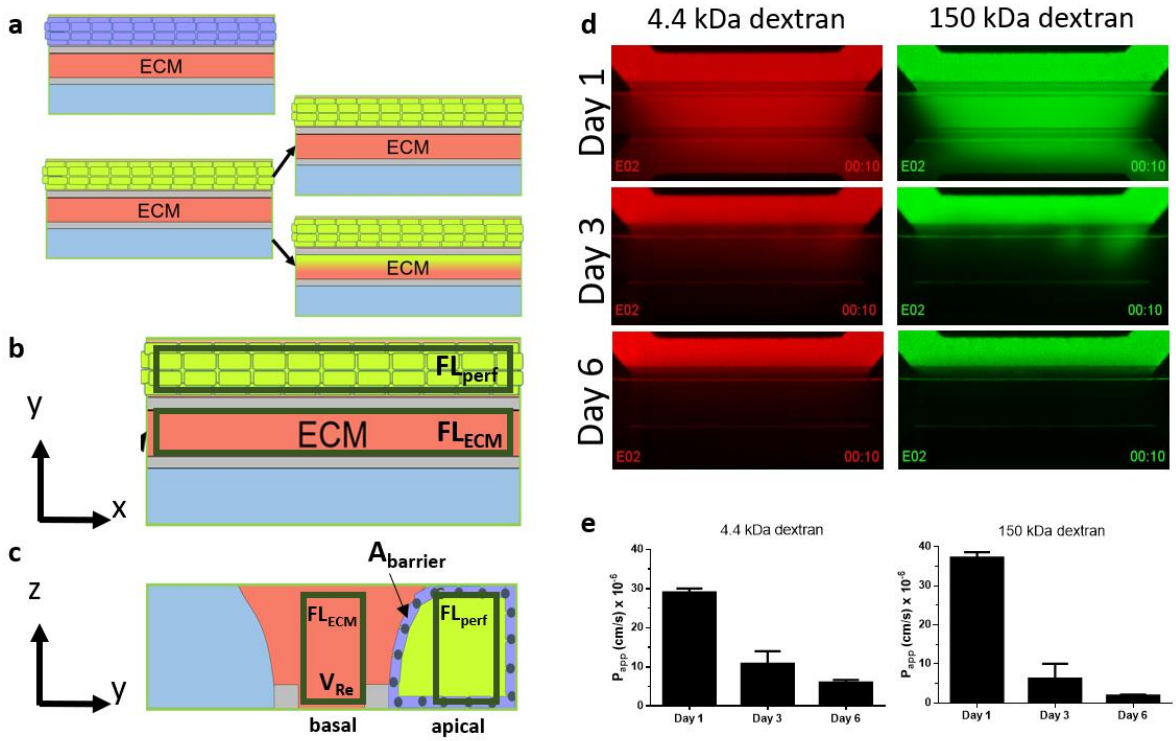

Figure 2: ***Barrier Integrity assay on tubular culture in the 3-lane OrganoPlate platform. a*** *The barrier integrity of the cell layer against the ECM was examined by perfusing the lumen of the tubule with dextran dyes. In healthy, leak-tight tubules dyes remain in the lumen, whereas in leaky tubules the dye enters the ECM channel.* ***b*** *The proportion of dye leaking through the tubule was monitored by measuring the fluorescence of the leaking dye into the gel. The gel channel intensity (FL_{ECM}) was normalized for the intensity of dye in the perfusion channel (F_{Lperf}).* ***c*** *Vertical illustration of the dye in the lumen of the tubule. $A_{barrier}$ is the area of the cell layer against the interface, $V_{receiver}$ (V_{re}) is the volume of the ECM behind the barrier which receives the dye.* ***d*** *Fluorescent images of the 10 minutes timepoint. Images were taken at day 1, day 3, and day 6 after seeding of RPTEC. At day 1 tubules did not form a barrier yet, whereas at day 3 the barrier is already partially formed. From day 6 the barrier is leak tight.* ***e*** *Apparent permeability (P_{app}) of the RPTEC tubules at different days. For all measurements, the same chips were analyzed over time (n=4). Error bars represent the standard deviation.*

Cisplatin exposure

To determine the toxic effect of cisplatin on RPTEC tubules in the OrganoPlate medium of both channels (apical and basal) was replaced at day 6 after seeding with TOX medium (MEME alpha Modification (Sigma, M4526) supplemented with RPTEC Tox Supplement (Sigma, MTOXRTSUP), L-glutamine (1.87 mM, Sigma, G7513)) in the presence of 0, 5, 15, 30, 90, 135, or 270 µM cisplatin (Sigma, P4394, stock: 5 mM in 0.9 % NaCl (Sigma, S7653) in H_20). After 48-hour incubation on the rocker platform phase contrast images were taken and medium was sampled from the top channel. Samples from in- and outlet were pooled and used for the LDH activity assay. Next, tubes

were incubated with WST-8 to determine cell viability. The barrier integrity of the exposed tubules was assessed consecutively of the WST-8 assay. After the exposures and viability measurements, the tubules were fixed with formaldehyde and stained with H2A.X, actin and ZO-1.

Lactate Dehydrogenase Activity Assay

Lactate dehydrogenase (LDH) activity of the samples was determined using the Lactate Dehydrogenase Activity Assay Kit (Sigma, MAK066) according to manufacturer protocol. In short: The medium of the top in- and top outlet was pooled and 2 µL was added in duplicate to a 384 well plate. In parallel a concentration curve of the NADH standard was added. Next, 18µL LDH Assay Buffer was added to all sample wells to bring to an initial volume of 20µl. After a short centrifugation of the plate, 20µl Master Reaction Mix were added to each well and mixed on a horizontal shaker in the plate reader. After one minute, the absorbance was measured at 450 nm. While the plate was incubated it was measured every 2 minutes until the value of the most active sample was higher than that of the highest standard (12.5 nmol/well). For the analysis the LDH activity was determined using the following formula

$$\textbf{LDH activity} = \frac{\textbf{B x Sample Dilution Factor}}{(\textbf{Reaction time})\ \textbf{x V}}$$

Where B is the amount (nmole) of NADH generated between $t_{initial}$ and t_{final}, the reaction time is $t_{final} - t_{initial}$ (in minutes), and V is the sample volume (in mL) added to the well.

Cell viability (WST-8 assay)

The cell viability of the cells was determined using the Cell Counting Kit – 8 (Sigma, 96992). The WST-8 solution was diluted 1:11 with TOX medium and added to the channels of the OrganoPlate (30 µL in- and outlets). After 18 minutes on the rocker platform and a 2-minute flat incubation, the absorbance in the top in- and outlets was measured with the Multiskan™ FC Microplate Photometer (Thermo scientific) at 450 nm.

Calcein-AM efflux inhibition

Medium in all perfusion channels was replaced with 1 µM calcein-AM (Life technologies, C3099, stock: 1 mM in DMSO) in KHH buffer (Krebs-Henseleit (Sigma, K3753) + 10 mM HEPES (Gibco, 15630) adjusted to pH 7.4) in the presence of 10 µM cyclosporin A (Sigma, 30024, stock: 5 mM in DMSO), 500 µM Digoxin (Fluka, 4599, stock: 100 mM in DMSO), or 0.5% DMSO (Sigma, D8418, vehicle control). After a 60 minutes incubation on the rocker platform chips were washed one time with ice cold KHH buffer. In the next washing step Hoechst 33342 (2 drop/ml, Life Technologies, R37605), 10 µM PSC833 (Sigma, SML0572, stock: 5 mM in DMSO), 10 µM Ko143 (Sigma, K2144, stock: 10 mM in DMSO), and 10 µM MK571 (Sigma, M7571, stock 10 mM in H_2O) were added to the washing solution and the plate was imaged with the ImageXpress® Micro Confocal High-Content Imaging System.

MRP2/4 efflux inhibition

Medium in all perfusion channels was replaced with 1.25 µM CMFDA (Molecular Probes, C7025, stock: 2.5 mM in DMSO) in the presence of 0, 10, 20, and 30 µM MK571 (Sigma, M7571, stock 10 mM in H_2O) in KHH buffer. After 30 minutes incubation on the rocker platform the chips were washed one time with ice cold KHH buffer. In the next washing step Hoechst 33342 (2 drops/ml, Life Technologies, R37605), 10 µM PSC833 (Sigma, SML0572, stock: 5 mM in DMSO), 10 µM Ko143 (Sigma, K2144, stock: 10 mM in DMSO), and 10 µM MK571 (Sigma, M7571) were added to the washing solution and the plate was imaged with the ImageXpress® Micro Confocal High-Content Imaging System.

6-NBDG influx inhibition

Medium in the apical channel (fig. 1) was replaced with OptiHBSS (1/3 Opti-MEM (Gibco, 11058-021), 2/3 HBSS (Sigma, H6648)) containing 500 µM 6-(N-(7-Nitrobenz-2-oxa-1,3-diazol-4-yl)amino)-6-Deoxyglucose (6-NBDG, Molecular Probes, N23106, lot 1704487, stock 10 mM in H_2O) and 0, 20, 100, or 500 µM Phlorizin (Sigma, P3449, stock 200 mM in Ethanol (JT Baker, 8025.2500PE)). All conditions contained 0.25% Ethanol as vehicle control. Medium in the basal channel was replaced with 6-NBDG free medium, concentrations of phlorizin matched apical channel concentrations. After a 30 minutes incubation on the rocker platform cells were washed two times with ice cold OptiHBSS. In the second washing step Hoechst 33342 (2 drops/ml, Life Technologies, R37605) was added to the washing solution and the plate was imaged with the ImageXpress® Micro Confocal High-Content Imaging System.

Image acquisition and analysis of the transport experiments

For the in-cell transport assays plates were imaged with the ImageXpress® Micro Confocal High-Content Imaging System. A z-stack of 220 µm with 10 µm between each image plane was imaged with the FITC and the DAPI channel (fig. S1). The intensity of the FITC signal of the cells growing against the ECM was analyzed with Fiji [13] and corrected for the background and cell number. Treated chips were normalized against vehicle control.

Trans-epithelial transport assay

Medium in the apical channel was replaced with medium containing 20 µM cyclosporin A or 0.4% DMSO. Medium in the basal channel was replaced with TOX medium containing 10 µM Rhodamine 123 (Sigma, 83702, stock: 50 mM in Ethanol) together with 20 µM cyclosporin A or 0.4% DMSO. To determine the concentration of rhodamine 123 a concentration curve was added to unused chips. Tubules were incubated for 5 hours on the rocker platform. After 3 hours and after 5 hours rhodamine 123 concentration was measured by imaging the top inlets with the FITC filter on the ImageXpress Micro XLS-C High Content Imaging Systems. The apparent permeability (P_{app}) was calculated by using the formula

$$P_{app} = \frac{\Delta C_{receiver} \times V_{receiver}}{\Delta t \times A \times C_{donor}} \left(\frac{cm}{s}\right).$$

$C_{receiver}$ is the measured intensity difference in the top wells between t_{3h} and t_{5h}, $V_{receiver}$ is the receiving volume in the reservoirs of the top inlets, t is the time difference t_{5h}-t_{3h} = 2 hours, A is the surface of the ECM interface with the medium channel, and C_{donor} is the donor concertation of 10 µM rhodamine 123.

Flow simulation and experimental verification

The platform described in this work uses a gravity-based perfusion system. The fluid flow rate and induced shear stress in the microfluidic channels of the OrganoPlate was estimated using a numerical model simulated in Python (Python Software Foundation, USA). This model calculates the induced pressure difference between two volumes of fluid, which are present in two microtiter plate wells that are connected by a microfluidic channel. The numerical model is described in more detail in the supplementary information. To validate the numerical model the gravity driven flow in the OrganoPlate, absorption was sequentially measured at 494 nm using a Fluorescein solution (Sigma, 46960, 10 µg/ml in water). For the verification a 9603200B OrganoPlate (2-lane plate with 120 x 200 µm, w x h channels) was used. The FITC solution was added to the channel system with 50 µL in each in- and outlet. After tilting the plate at a set angle the fluorescence of both wells was measured and compared with the associated simulated volumes.

Statistics and data analysis

Images were analyzed using Fiji [13]. Data analysis was performed using Excel (Microsoft office 2016) and GraphPad Prism (GraphPad Software Inc., version 6.07). Error bars represent the standard deviation. Data were analyzed using one- way ANOVA followed by a Dunnett multiple comparison test which compares all treated chips to the control chips. Comparisons of two groups were done using the t-test. A p-value of < 0.05 was considered to be significant. At least 3 technical replicates per data point were obtained.

Results

Development of a proximal tubule-on-a-chip

The platform we used to develop perfused 3D proximal tubules was the 3-lane version of the OrganoPlate (fig. 1a). The top part of this plate is a standard 384-well plate with a modified glass bottom. In the bottom of the OrganoPlate, 40 microfluidic chips are embedded. One chip consists of three 400-µm-wide and 220-µm-high channels separated by ridges, the phaseguides [14]. First, an extracellular matrix (ECM) gel was loaded to the middle channel of the OrganoPlate. The liquefied ECM entered the channels by capillary action and did not overflow to the adjacent channel through meniscus pinning on the phaseguide. The ECM is free-standing, allowing interrogation of the epithelial barrier function without interference of an artificial membrane. For the seeding procedure, a single cell suspension of RPTEC was added to one of the adjacent channels and cells could attach to the ECM by placing the plate on its side, in vertical position (fig.

1a). After attachment of the cells, the plate was placed flat on a rocking platform. By positioning the in- and outlets of one chip on different heights, liquid flow was induced through the channels by leveling between the reservoirs (fig. S5a). Fluid flows are bidirectional and pulsatile. Flow profiles have been simulated and experimentally verified (fig. S5b). The change in fluorescence due to flow of FITC solution between wells showed a high correlation with the associated simulated volumes. Results show that mean flow rates of 2.02 µL/min could be achieved with a mean shear of 0.13 dyne/cm^2 (fig. S5 c,d).

The seeding and culture conditions for proximal tubules-on-a-chip based on RPTEC cells were optimized by testing different settings for parameters, such as seeding density, ECM composition, medium composition, and perfusion height and angle. Figure 1b shows optimal tube formation of RPTEC over time. As seen in figure S3 the flow is crucial for the tubule formation. Without any flow, tubule formation is not possible. In figure S4 the long-term viability of the RPTEC in the OrganoPlate is depicted. RPTEC are stable in the OrganoPlate up to day 11. After this time period, cells start invading the ECM which makes barrier dependent assays impossible. Therefore, it was decided to perform all assays from day 6 to day 10.

Proximal Tubules-on-a-chip form polarized tight barriers

RPTEC tubules were cultured in the OrganoPlate for 7-10 days. As depicted in figure 1c, RPTEC formed a tubular structure with cells lining the ECM (curved part of the tubule) and the walls of the channel, thus having an open, perfused lumen. Confluent tubules formed tight-junctions as visualized by the zona-occludence 1 tight junction (ZO-1) expression [15], and display primary cilia visualized by acetylated tubulin staining [16]. A single cilium per cell was observed, located at the apical side of the cell layer pointing towards the lumen of the tubule (fig. 1c,d). The tubules were also stained for Ezrin [17] that was expressed on the luminal side of the tubule (fig. 1d). It is thus confirmed that the tubes are polarized in a correct manner, with the lumen being the apical side (corresponding to the pre-urine side in an *in vivo* situation) and the basal side being against the extracellular matrix (corresponding to the blood side in and *in vivo* situation).

Subsequently, the integrity of the epithelial barrier was investigated. To this end, a fluorescently labeled dextran was administered to the lumen of the tube. Leakage of the fluorescent dextran from the perfusion channel into the gel compartment was monitored and quantified in order to have a measure for the integrity of the epithelial cell monolayer (fig. 2a-c). To monitor the tubule formation over several days, a higher molecular weight dextran (150 kDa FITC) and a lower molecular weight dextran (4.4 kDa TRITC) were used and leakage was assessed at day 1, 3, and 6 days after seeding. At day 1, no barrier formation could be detected, whereas at day 3 the tubes were partly leak-tight. At day 6, the tubules were fully leak-tight for both dyes (fig 2d). After quantification of the signal at day 6, the calculated P_{app} (apparent permeability) of the tubules were 6 x 10^{-6} cm/s for the 4.4 kDa dextran and 2 x 10^{-6} cm/s for the 150 kDa dextran (fig. 2e). A good barrier integrity of the tubule is crucial for assessing transport and directional toxicity as it

allows interrogation and exposure of the apical and basolateral sides in independently from one another.

The proximal tubule-on-a-chip allows nephrotoxicity assessment

Next, kidney tubules were assessed for toxicity response to cisplatin. Cisplatin is an anti-cancer drug, which is used for the treatment of tumors of the lung, ovary, testicles, and head and neck [18]. The main route of the excretion of cisplatin is via the proximal tubules, which leads to a higher accumulation of the drug in the cells compared to other organs [19]. Kidney tubules were exposed six days after seeding for 48 hours to cisplatin at concentrations ranging from 5 to 270 µM. The toxic effect of cisplatin on the proximal tubules was determined through multiplexing several assays: phase contrast imaging, barrier integrity assessment, WST-8 viability measurement, LDH release and immunohistochemical staining of tight junctions, DNA damage and cytoskeleton integrity. The morphology of the tubules was analyzed by phase contrast imaging and visually started to change at 270 µM cisplatin concentration, at lower concentrations no significant differences were observed (fig. 3a). Cisplatin showed a dose-dependent disruption of the barrier integrity of the tubes as determined by leakage of fluorescent dextran 4.4 kDa and 150 kDa (fig 3b,c) with a matching increase in calculated P_{app} for both the small and large dextran (fig. 3d).

In addition to measuring the impairment of the barrier integrity of the tubules, the cell viability was assessed using the live cell enzymatic activity WST-8 assay. A decrease in cell viability was observed at cisplatin concentrations of 30 µM and higher, which was reduced to approximately 76% compared to the vehicle control at the highest concentration of 270 µM (fig. 3e). Consistent with this, a significant increase in LDH (lactate dehydrogenase) release into the lumen was detected at cisplatin concentrations of 30 µM and higher (fig. 3f). Immunohistochemical analysis of the exposed tubules further confirmed the toxicity of cisplatin. At concentrations of 30 µM and higher, cisplatin caused increased DNA-damage (detected by H2A.X DNA-damage marker staining [20], Fig. 3g,h) and reduced expression of ZO-1 protein in the tight junctions (fig. 3g and 3j). Changes in the actin cytoskeleton were observed from 5 µM onwards (fig. 3g,i).

Active substrate transport across the epithelial membrane

The kidneys play a crucial role in eliminating drugs and metabolic waste products through excretion into the urine [21]. Many compounds require active transport by dedicated enzymes, the efficiency of which can be compromised by different drugs [2], [22].

To study the transporter functionality of kidney tubules in the OrganoPlate, calcein-AM and CMFDA were used to monitor P-gp and MRPs, respectively. These two transporters, that transport substrates into the apical lumen, are from the ATP-binding cassette family of transporters. P-gp mainly transports cationic as well as unconjugated xenobiotics whereas MRP is responsible for removing conjugated compounds from the body [22], [23].

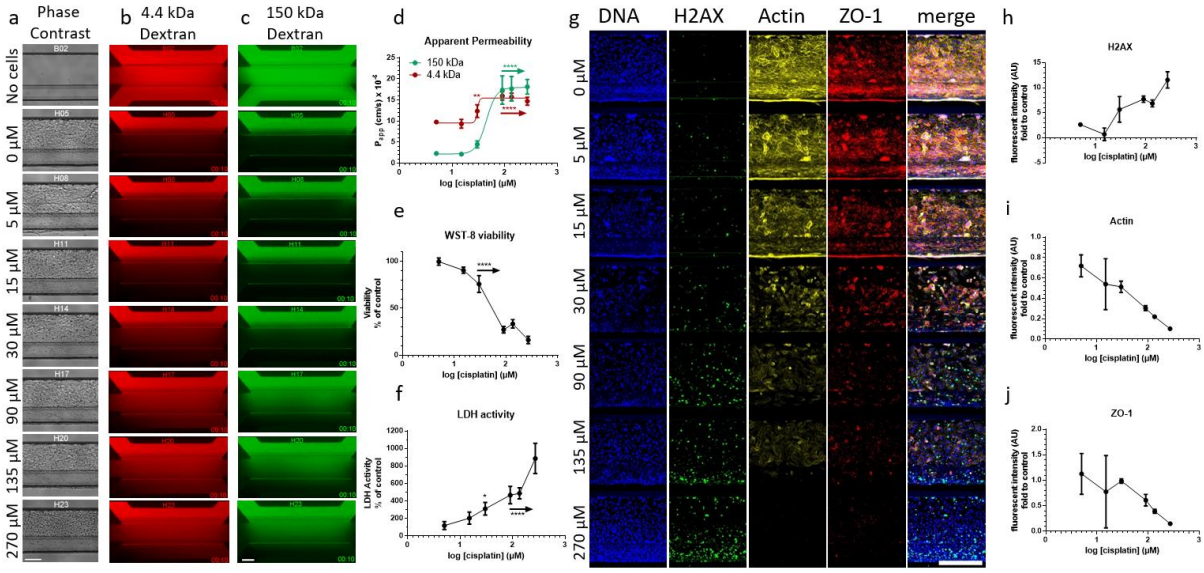

Figure 3: Toxicant readouts after 48 hours cisplatin exposure*. a visual break down of the tube after 48h treatment at highest concentrations. Scale bar = 100 µm. b-c Perfusion of the lumen in the top channel with a lower sized dextran dye of 4.4 kDa and a higher sized dextran dye of 150 kDa. From a concentration of 90 µM the ECM behind the barrier is filled with dye, whereas at concentrations of 5 µM and 15 µM no difference compared to vehicle control can be seen. Scale bar = 200 µm. d For quantification of the barrier function the apparent permeability (Papp) was calculated. For both dextran sizes a significant increase of the Papp could be detected from 90 µM ($p<0.0001$) compared to vehicle control. e To quantify viability of the cells a WST-8 assay was used. WST-8 is reduced by the cells to an orange formazan product which can be measured with an absorbance reader at 450 nm. Viability was significantly reduced ($p<0.0001$) from 30 µM compared to vehicle control. f LDH activity in the medium indicated the number of dead cells. The LDH assay detected, similar to the WST-8 assay a significant effect of cisplatin from 30 µM ($p<0.05$). g Maximum projections or the Immunostaining against H2A.X (DNA damage), actin (cytoskeleton) and ZO-1 (tight junction marker). Scale bar = 200 µm. h-j Fluorescent intensity analysis of the summary projections of DNA damage marker H2A.X, actin cytoskeleton marker, and tight junction marker ZO-1. The intensity of all three markers is corrected for the background and nuclei count. Graphs show data of 3 chips per condition. Error bars represent the standard deviation.*

Calcein-AM is a substrate for P-gp which is often used to assess the functionality of the transporter [23]. Cell tracker reagent 5-chloromethylfluorescein diacetate (CMFDA) is a compound for the MRP transporters [24]. Both compounds enter the cells passively and are converted inside of the cells to the green fluorescent dyes calcein and GS-MF, respectively [23], [25]. Cyclosporin A is an inhibitor of the P-gp transporter, whereas digoxin, which is a medication used to treat various heart conditions, is a substrate for P-gp [2] (fig. 4a). MK571 is an inhibitor of the MRPs [2] (fig 4d).

To measure the influence of compounds on transport activity in the proximal tubule-on-a-chip we set up fluorescent substrate-based activity assays (fig. S1). For the analysis of the uptake of fluorescence inside of the cells lining the ECM, a z-stack of the tubule was imaged, and planes of the desired area are selected (fig. S1e). After removal of the signal from out-of-focus cells, stacks were compressed, and the signal was integrated (fig. S1f).

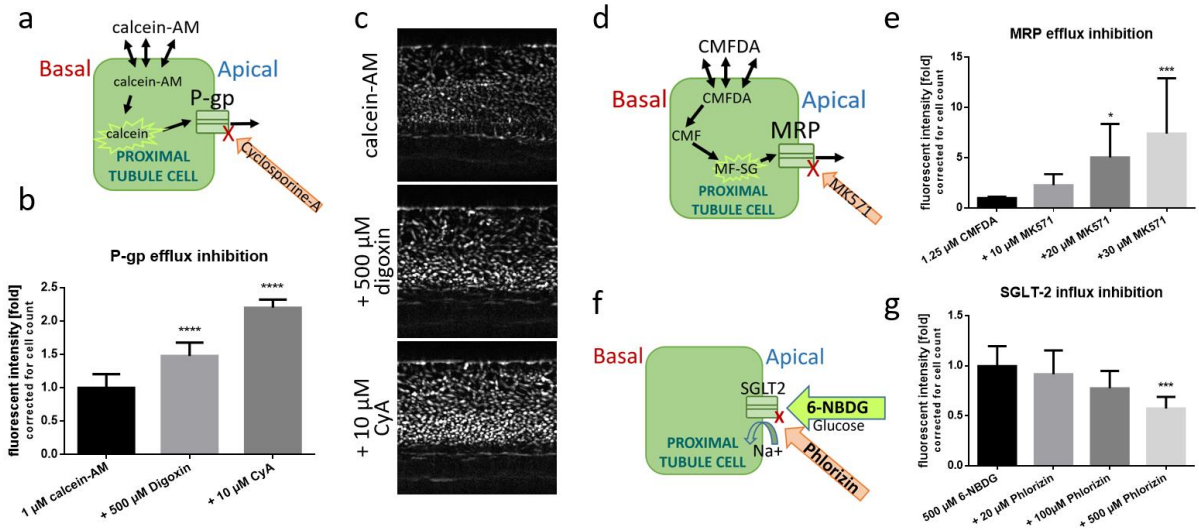

Figure 4: ***Evaluation of P-gp, MRP and SLGT2 transporter activity in proximal tubule-on-a-chip. a*** *When the non-fluorescent calcein-AM enters the cell membrane esterases in the cytoplasm cleave the acetoxymethyl (AM) ester group, which results in fluorescent calcein. Calcein-AM is pumped out of the cell by the P-glycoprotein-transporter (P-gp).* ***b*** *Inhibition of calcein-AM efflux: RPTEC were incubated for one hour with 1 µM calcein-AM ± inhibitors. 10 µM cyclosporin A showed the highest inhibitory effect followed by 500 µM digoxin.* ***c*** *Z-Projections of representative images of the calcein-AM exposed RPTEC area. A higher fluorescent signal could be observed in the presence of transport inhibitors. Scale bar = 200 µm.* ***d*** *Similar to calcein-AM non-fluorescent CMFDA enters the cells passively. Inside the cells CMFDA is transformed to fluorescent MRP substrate GS-MF.* ***e*** *Dose-dependent efflux inhibition of GS-MF by MK571 resulted in a significant increase of fluorescent signal inside the cells.* ***f*** *Influx of fluorescent glucose analog 6-NBDG is inhibited by phlorizin. 6-NBDG influx is mediated by the sodium dependent SGLT2 transporter.* ***g*** *6-NBDG influx into RPTEC was significantly inhibited by 500 µM phlorizin and a dose dependent trend was observed when inhibited with 20 and 100 µM phlorizin. **: p<0.01 ***: p<0.001 and ****: p<0.0001 one-way Anova with Dunnett's comparison test. Each of the three graphs shows combined data of two independent experiments with 2-5 chips per condition. Error bars represent the standard deviation.*

As both dyes enter the cells passively, RPTEC tubules were exposed to the dyes as well as their respective inhibitors from the apical as well as basal side. A 2.2 ± 0.1 or 1.5 ± 0.2 fold increase in calcein accumulation was observed after co-incubation with cyclosporin A or digoxin, respectively, confirming P-gp activity as both drugs competitively interact with the efflux pump (fig. 4b-c). To monitor MRP-function, an efflux inhibitor cocktail of PSC833, MK571 and Ko143 was used to avoid redundancy of other transporters [23]. A dose-dependent inhibition of GS-MF efflux was observed upon increasing MK571 concentrations, as shown in Figure 4e, confirming MRP activity.

In addition to the efflux transporters, the glucose uptake by the sodium-glucose linked transporter SGLT2 [26], [27] was evaluated using the fluorescent glucose analogue 6-NBDG [28]. SGLT2-mediated influx from tubular lumen into the cells was sensitive to inhibition by the SGLT inhibitor phlorizin [29] (fig. 4f-g). This confirms the presence and activity of the SGLT2 transporter.

The proximal tubule-on-a-chip allows transepithelial transport assessment

To further examine the capability of transepithelial transport across the epithelium of the 3D perfused proximal tubules, the flux of rhodamine123 from the basolateral to the apical compartment was assessed. Rhodamine123 is a substrate of P-gp and its transport was analyzed in absence and presence of the transport inhibitor cyclosporin A [30].

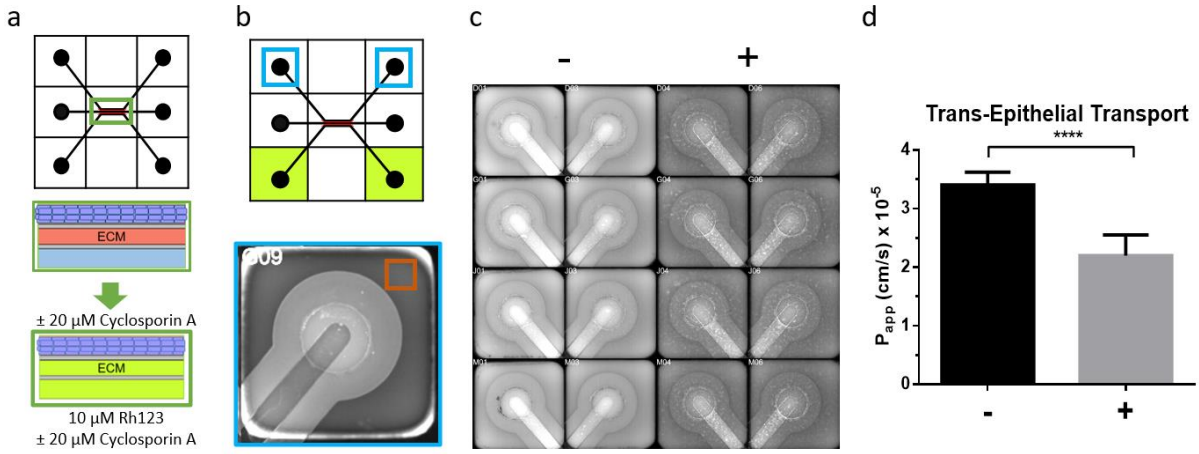

Figure 5: Transepithelial transport of rhodamine 123*. a 10 µM rhodamine 123 was added solely to the basal side of the tubule with or without 20 µM cyclosporin A present at both sides of the tube. b After 3 and 5 hours images were taken from the inlets guiding to the lumen of the tubule (blue squares: measured wells). The intensity above the glass bottom of the wells was measured (orange square: area selection). To determine the concentration of rhodamine 123 in the top wells, spiked samples were added to empty chips on the same plate and analyzed. The resulting concentrations were used to calculate the Papp of the transport of rhodamine 123. c Images of the top in- and outlets or the OrganoPlate show the apical fluorescent signals after 5-hour incubation of rhodamine 123 on the basal side of the tubule. A decreased fluorescent signal was observed after co-incubation with cyclosporin A, as shown in the top inlets. -: without transport inhibition, +: with 20 µM cyclosporin A addition (apical and basal). d A significant decrease in Papp was observed when adding rhodamine 123 together with 20 µM cyclosporin A. ****: p<0.0001. Data are combined from two independent experiments with 5-9 chips per plate and per condition. Error bars represent the standard deviation.*

The experimental set-up is shown in Figure 5a-b. Rhodamine123 was administered to the basal perfusion channel and measured in the perfusion medium on the apical side. In order to have a highest signal-to-noise ratio, the fluorescent signal was measured in apical-side in- and outlet, where the liquid column was largest. Inhibition of transport by cyclosporine A reduced fluorescence signal in the apical-side in- and outlets as shown by representative images in Figure 5c. It is known that cyclosporin A has a toxic effect on the kidney. Therefore, its effect on the barrier integrity was assessed. It was found that a concentration of 20 µM cyclosporin A was determined as safe as transport inhibitor, supported by the absence of an effect on barrier integrity (fig. S2). The P_{app} of rhodamine123 changed from $3.4*10^{-5} \pm 0.1*10^{-5}$ cm/s without inhibitor to $2.2*10^{-5} \pm 0.1*10^{-5}$ cm/s with cyclosporin A, indicating (inhibition of) active transport (fig. 5d). This is a clear demonstration that transepithelial transport can be assessed in the system.

Discussion & Outlook

We reported the development of a functional proximal tubule-on-a-chip model which can be implemented for routine assessment of kidney toxicity and drug-drug interaction studies. The OrganoPlate platform allows parallel culture and assessment of 40 independent kidney tubules. This is important in toxicological studies or in compound testing as it allows for proper controls, replica's and dilutions series. Induction of flow is realized by passive leveling on an interval rocker system, which is an easy to use alternative to complex pump solutions. Other than the rocking platform, no further specialized lab equipment is needed. As the format of the platform is a standard microtiter layout of a 384 well plate it is fully compatible with most readers, microscopes and robot handling equipment. The platform is fully pipet operated and media changes as well as reagent additions are non-invasive. Physiologically relevance of the system is enhanced by culturing epithelial cells directly against an extracellular matrix mimic in a manner that is free of artificial membranes, under application of perfusion flow and by mimicking the 3D morphology.

A critical aspect in the concept is the selective patterning of extracellular matrix in the chips. In order to do this surface tension techniques have been employed that allow selective ECM priming using pipetting means only. As a consequence thereof, only part of the tube is exposed to the ECM (curved part).

This does not hamper the measurement results as the barrier and the rhodamine transport assay exclusively consider the cell layer against the extracellular matrix. Other systems are known from literature that have full ECM embedment [31], however, such systems come at the cost of throughput and ease of handling, as it is impossible to create a lumen in an ECM gel with pipetting steps only.

Similar choices were made with respect to the dimensions of the proximal tubule. In this study the diameter of the tubules are 400 µm, which is significantly larger than the *in vivo* proximal tubules (approximately 60 µm [32]). However, the choice for larger dimensions allowed a greater sensitivity of assays, particularly those that are executed off chip.

We showed the multiplexing assays in a microfluidic format. The barrier integrity could be monitored in real time by adding a reporter dye. In parallel cellular enzymatic activity (WST-8) and LDH release could be measured. All three assays yielded a similar result to cisplatin exposure, indicating the robustness of the model. Immunohistochemical staining was also used in a multiplex manner for assessment of the effect of cisplatin on the tight junctions (ZO-1), cytoskeleton (actin) and DNA damage (H2A.X). Although some showed higher sensitivity than the live assays, the stains represent an end-point assay and require much more effort to execute properly. Moreover, only a limited number of stains could be multiplexed in the same model, requiring replica's to be used for different analyses.

The multiplexed live assays used for acute kidney toxicity detection here are compatible with chronic toxicity assessments. For example the barrier integrity assays was previously used to study 5-days exposure of gut tubules to toxicants [33]. Non-invasive assays are important to study chronic effects of drugs that only exert negative effects after prolonged use. The proximal tubule model developed here together with multiplexed assays and the possibility for repeated dosing of the model allows for future longitudinal studies.

In this publication we used the microfluidic system for growing tubular structures. In addition to that, other cell types can be embedded into the ECM. An example of functional 3D networks of neurons and glia embedded in the ECM of one channel with an adjacent medium channel is shown by Wevers et al. [34] and Lanz et al. studied the behavior of breast cancer cells grown in an ECM [35]. The method of culturing cells embedded in the ECM can be easily combined with the model presented here: instead of culturing the RPTEC against a pure ECM, supporting cells can be added into the ECM. In addition to this the complexity of the model could be further increased by growing an endothelial tubule in the basal-side perfusion channel. Ultimately, we aim to combine endothelium, fibroblasts and podocytes to have a fully functional kidney-on-a-chip model.

We showed two different possibilities to monitor the transport of the proximal tubules. First, we measured and analyzed the signal of compounds retained by the cells lining the ECM layer. Second, we showed feasibility of transepithelial transport studies on the RPTEC containing tubules using the fluorescent substrate, rhodamine123. Both types of experiments show clear transporter functionality, whereas the latter is the most complex functional assay. We have not assessed organic anion transporter (OAT) expression by the RPTEC used in this study, but 2D evaluation by Suter-Dick [36] showed no response to Tenofovir, indicating absence of the OAT1 transporter. This limits the use of the cell line for assessment of transport of organic ions. To compensate for this, we also implemented a cell line over expressing the organic anion transporter 1 (ciPTEC, [37]). In future work we will compare the performance of both cell models in response to a range of blinded compounds.

For future studies, transport capabilities will be shown also for non-fluorescent substrates. To achieve this goal, radiolabeled compounds or mass spectrometry can be used to analyze and quantify transport. In this manner a much wider range of compounds and transporter functionality can be investigated. These off-plate assays will require sampling of the perfusate instead of the microscope-based read outs used here. The use of microfluidic chips requires limited amounts of cells and medium, which is positive in the light of use of valuable materials with restricted access. However, for certain analysis methods the small sample volumes could be limiting. Detection of transported compounds will depend on the sensitivity of the analysis method (e.g. mass spectrometry). Other off-plate analyses as e.g. qRT-PCR are feasible through pooling of chip lysates. Such functional assays will be of great support for *in vitro* to *in vivo* extrapolation.

In summary we developed a user-friendly, functional kidney-on-a-chip model that can be used to study the effect of compounds in 40 parallel cultured renal tubules. The tubules could be assessed for barrier function by fluorescent imaging and multiplexed with a range of assays including viability, LDH leakage and immunohistochemical staining. In addition, transporter activity was shown by means of transport inhibition studies for both substrate uptake, as well as transcellular transport. The functionality of the platform in combination with the ease of handling and decent throughput makes this a useful platform for studying nephrotoxicity, compound excretion, drug-drug interaction studies and disease mechanisms.

Acknowledgements

This project was financially supported by NC3Rs (National Center for the Replacement, Refinement and Reduction of Animals in Research), UK; under the Crack-it challenge 15 (Nephrotube, project no. 37497-25920). We thank Professor Dr Hans Tanke for the use of the imaging facilities at the Department of Molecular Cell Biology, Leiden University Medical Center, and Joop Wiegant and Annelies van der Laan for their assistance.

Regarding originality and conflict of interest

This publication contains original work. The authors M.K. Vormann, L.Gijzen, S. Hutter, L.Boot, A.Nicolas, A. vd Heuvel, B. de Wagenaar, J. Joore, P.Vulto, and H.L. Lanz are or were employees of Mimetas B.V. This affiliation is declared. The OrganoPlate® is a registered trademark of MIMETAS BV.

References

[1] Lauralee Sherwood, *Human Physiology: From Cells to Systems*. Brooks Cole, 1997.

[2] K. M. Morrissey, S. L. Stocker, M. B. Wittwer, L. Xu, and K. M. Giacomini, "Renal Transporters in Drug Development," *Annu. Rev. Pharmacol. Toxicol.*, vol. 53, no. 1, pp. 503–529, 2013.

[3] M. J. Wilmer, C. P. Ng, H. L. Lanz, P. Vulto, L. Suter-Dick, and R. Masereeuw, "Kidney-on-a-Chip Technology for Drug-Induced Nephrotoxicity Screening," *Trends Biotechnol.*, vol. 34, no. 2, pp. 156–170, 2016.

[4] K. A. Homan *et al.*, "Bioprinting of 3D Convoluted Renal Proximal Tubules on Perfusable Chips," *Sci. Rep.*, vol. 6, pp. 1–13, 2016.

[5] E. M. Vedula, J. L. Alonso, M. A. Arnaout, and J. L. Charest, "A microfluidic renal proximal tubule with active reabsorptive function," *PLoS One*, vol. 12, no. 10, pp. 1–15, 2017.

[6] K. J. Jang *et al.*, "Human kidney proximal tubule-on-a-chip for drug transport and nephrotoxicity assessment," *Integr. Biol. (United Kingdom)*, vol. 5, no. 9, pp. 1119–1129, 2013.

[7] Y. Qu *et al.*, "A nephron model for study of drug-induced acute kidney injury and assessment of drug-induced nephrotoxicity," *Biomaterials*, vol. 155, pp. 41–53, 2018.

[8] B. J. van Meer *et al.*, "Small molecule absorption by PDMS in the context of drug response bioassays," *Biochem. Biophys. Res. Commun.*, vol. 482, no. 2, pp. 323–328, 2017.

[9] V. van Duinen, S. J. Trietsch, J. Joore, P. Vulto, and T. Hankemeier, "Microfluidic 3D cell culture: From tools to tissue models," *Curr. Opin. Biotechnol.*, vol. 35, pp. 118–126, 2015.

[10] A. Junaid, A. Mashaghi, T. Hankemeier, and P. Vulto, "An end-user perspective on Organ-on-a-Chip: Assays and usability aspects," *Curr. Opin. Biomed. Eng.*, vol. 1, pp. 15–22, 2017.

[11] S. J. Trietsch, G. D. Israëls, J. Joore, T. Hankemeier, and P. Vulto, "Microfluidic titer plate for stratified 3D cell culture," *Lab Chip*, vol. 13, no. 18, pp. 3548–3554, 2013.

[12] S. Li *et al.*, "Development and Application of Human Renal Proximal Tubule Epithelial Cells for Assessment of Compound Toxicity," *Curr. Chem. Genomics Transl. Med.*, vol. 11, no. 1, pp. 19–30, Feb. 2017.

[13] J. Schindelin *et al.*, "Fiji: An open-source platform for biological-image analysis," *Nat. Methods*, vol. 9, no. 7, pp. 676–682, 2012.

[14] P. Vulto, S. Podszun, P. Meyer, C. Hermann, A. Manz, and G. A. Urban, "Phaseguides: A paradigm shift in microfluidic priming and emptying," *Lab Chip*, vol. 11, no. 9, pp. 1596–1602, 2011.

[15] B. R. Stevenson, J. D. Siliciano, M. S. Mooseker, and D. A. Goodenough, "Identification of Z0-1: a high molecular weight polypeptide associated with tight junction (zonula occludens) in a," *J. Cell Biol*, vol. 103, no. September, pp. 755–766, 1986.

[16] V. Raghavan and O. A. Weisz, "Flow stimulated endocytosis in the proximal tubule," *Curr. Opin. Nephrol. Hypertens.*, vol. 24, no. 4, pp. 359–365, 2015.

[17] M. Berryman, Z. Franck, and A. Bretscher, "Ezrin is concentrated in the apical microvilli of a wide variety of epithelial cells whereas moesin is found primarily in endothelial cells," *J. Cell Sci.*, vol. 105, no. 4, pp. 1025–1043, 1993.

[18] G. Giaccone, "Clinical perspectives on platinum resistance," *Drugs*, vol. 59, no. SUPPL. 4, pp. 9–17, 2000.

[19] G. S. Oh *et al.*, "Cisplatin-induced kidney dysfunction and perspectives on improving treatment strategies," *Electrolyte Blood Press.*, vol. 12, no. 2, pp. 55–65, 2014.

[20] L. J. Kuo and L.-X. Yang, "Gamma-H2AX - a novel biomarker for DNA double-strand breaks.," *In vivo*, vol. 22, no. 3, pp. 305–9, 2008.

[21] R. Masereeuw and F. G. M. Russel, "Regulatory pathways for ATP-binding cassette transport proteins in kidney proximal tubules," *AAPS J.*, vol. 14, no. 4, pp. 883–894, 2012.

[22] K. M. Giacomini *et al.*, "Membrane transporters in drug development," *Nat. Rev. Drug Discov.*, vol. 9, no. 3, pp. 215–236, 2010.

[23] P. Caetano-Pinto, M. J. Janssen, L. Gijzen, L. Verscheijden, M. J. G. Wilmer, and R. Masereeuw, "Fluorescence-Based Transport Assays Revisited in a Human Renal Proximal Tubule Cell Line," *Mol. Pharm.*, vol. 13, no. 3, pp. 933–944, 2016.

[24] S. E. Jenkinson, G. W. Chung, E. van Loon, N. S. Bakar, A. M. Dalzell, and C. D. A. Brown,

"The limitations of renal epithelial cell line HK-2 as a model of drug transporter expression and function in the proximal tubule.," *Pflugers Arch.*, vol. 464, no. 6, pp. 601–611, 2012.

[25] H. Lindenmaier, M. Becker, W. Haefeli, and J, "Interaction of progestins with the human multidrug resistance-associated protein 2 (MRP2)," *Drug Metab.*, vol. 33, no. 11, pp. 1576–1579, 2005.

[26] I. S. Wood and P. Trayhurn, "Glucose transporters (GLUT and SGLT): expanded families of sugar transport proteins," *Br. J. Nutr.*, vol. 89, no. 1, pp. 3–9, 2003.

[27] V. Vallon *et al.*, "SGLT2 mediates glucose reabsorption in the early proximal tubule," *J. Am. Soc. Nephrol.*, vol. 22, no. 1, pp. 104–112, 2011.

[28] D. W. Jung, H. H. Ha, X. Zheng, Y. T. Chang, and D. R. Williams, "Novel use of fluorescent glucose analogues to identify a new class of triazine-based insulin mimetics possessing useful secondary effects," *Mol. Biosyst.*, vol. 7, no. 2, pp. 346–358, 2011.

[29] J. R. L. Ehrenkranz, N. G. Lewis, C. R. Kahn, and J. Roth, "Phlorizin: A review," *Diabetes. Metab. Res. Rev.*, vol. 21, no. 1, pp. 31–38, 2005.

[30] F. J. Sharom, "The P-glycoprotein multidrug transporter," *Gen. Pharmacol.*, vol. 27, no. 8, pp. 1283–1291, 2011.

[31] E. J. Weber *et al.*, "Development of a microphysiological model of human kidney proximal tubule function," *Kidney Int.*, vol. 90, no. 3, pp. 627–637, 2016.

[32] H.-G. Liebich, *Funktionelle Histologie der Haussäugetiere und Vögel: Lehrbuch und Farbatlas für Studium und Praxis*, 5th ed. Stuttgard: Schattauer, 2010.

[33] S. J. Trietsch *et al.*, "Membrane-free culture and real-time barrier integrity assessment of perfused intestinal epithelium tubes," *Nat. Commun.*, vol. 8, no. 1, pp. 1–7, 2017.

[34] N. Wevers *et al.*, "3D networks of iPSC-derived neurons and glia for high-throughput neurotoxicity screening," *Toxicol. Lett.*, vol. 258, p. S157, 2016.

[35] H. L. Lanz *et al.*, "Therapy response testing of breast cancer in a 3D high-throughput perfused microfluidic platform," *BMC Cancer*, vol. 17, no. 1, p. 709, 2017.

[36] L. Suter-Dick *et al.*, "Combining Extracellular miRNA Determination with Microfluidic 3D Cell Cultures for the Assessment of Nephrotoxicity: a Proof of Concept Study," *AAPS J.*, vol. 20, no. 5, pp. 1–9, 2018.

[37] J. Vriend *et al.*, "Screening of Drug-Transporter Interactions in a 3D Microfluidic Renal Proximal Tubule on a Chip," *AAPS J.*, vol. 20, no. 5, 2018.

Supplementary Material

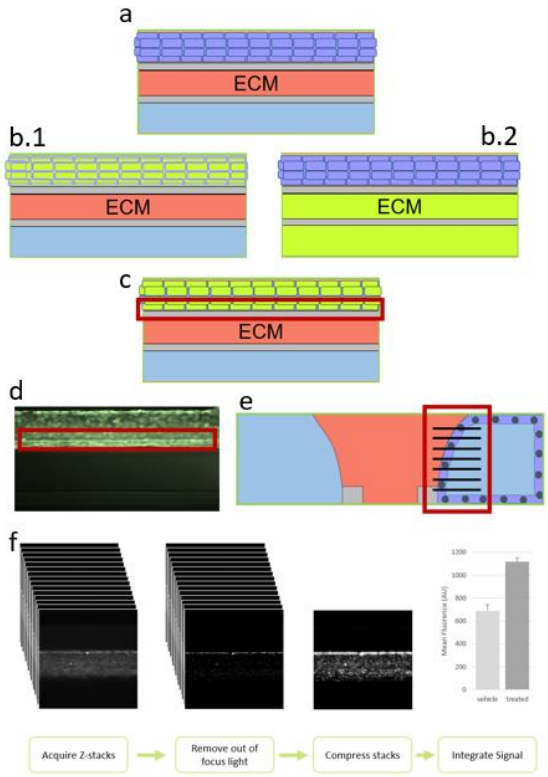

Supplementary figure S1: Cellular transport assay. ***a*** *Perfused tubules in the top channel of the OrganoPlate.* ***b*** *Exposure of the tubule with a fluorescent compound either transported through influx transporters into cells, or by efflux transporters out of cells. Both transport mechanisms can be inhibited by specific inhibitors.* ***b.1*** *Apical exposure with fluorescent compound from the apical side (inside of the tubule).* ***b.2*** *Basal exposure from the basal side of the tubule.* ***c*** *Self-fluorescent compounds need to be washed out of the ECM, whereas compounds which are only fluorescent in the cells can be measured without washing. Compound retention in the cells is measured in the cells against the ECM surface (red square).* ***d*** *Fluorescent image of a tube with a green fluorescent compound retained in the cells.* ***e*** *Vertical illustration of the area imaged for the analysis. The black stripes indicate the planes of the z-stack images.* ***f*** *Image analysis: z-stack of the tubule is acquired, and the out of focus light is removed. Subsequently the stack is compressed, and the intensity of the image is measured. After blocking the transport of the compound, the nuclei of the cells are stained and the FITC signal is corrected for the nuclei count.*

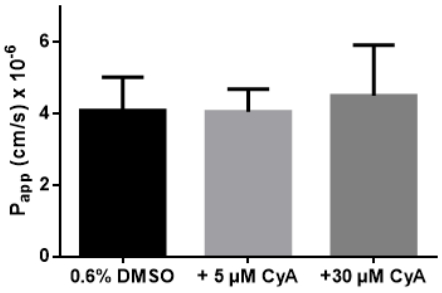

***Supplementary figure S2: Apparent permeability (Papp) after cyclosporin A exposure**. RPTEC tubules were exposed for 24 hours to 5 µM and 30 µM cyclosporin A. Both concentrations did not show a significant increase of the Papp after exposure. Each error bar represents the standard deviation of 4-5 chips.*

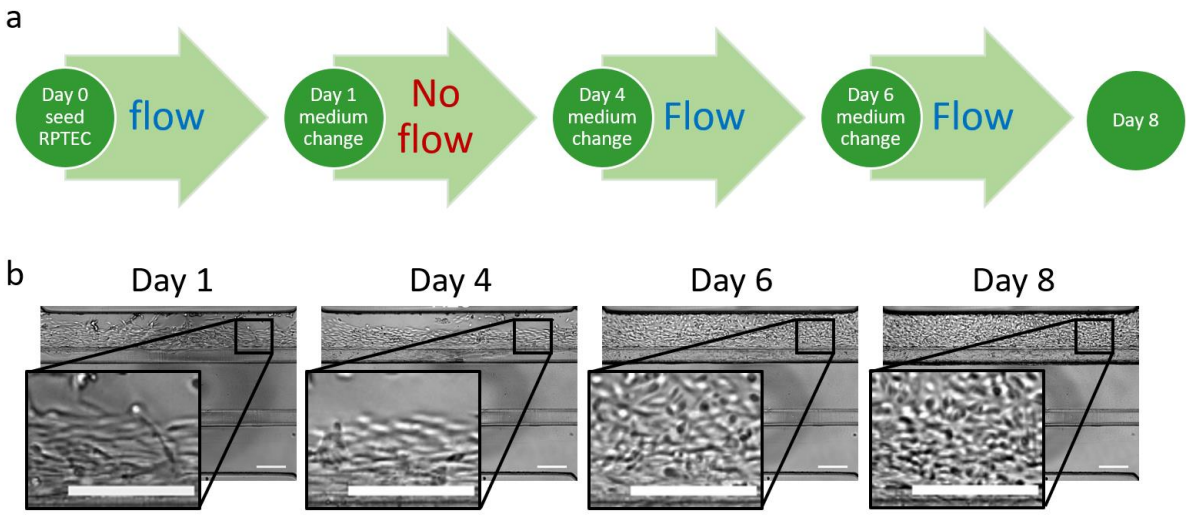

***Supplementary figure S3: Importance of flow for tube formation.** a Tubules were seeded and kept on the rocker platform for 24h hours. From day 1 to day 4 no flow was applied. The plate was placed back on the rocker platform from day 4 to 8. b Culturing the tubules without flow resulted in a lack of tubule formation at day 4 compared to the standard condition with flow (see fig. 1b). After reintroduction of flow the tube formation process recovered which resulted in a fully-grown tubule at day 8 (instead of day 6 as shown in fig. 1b). Scalebars = 200 µm.*

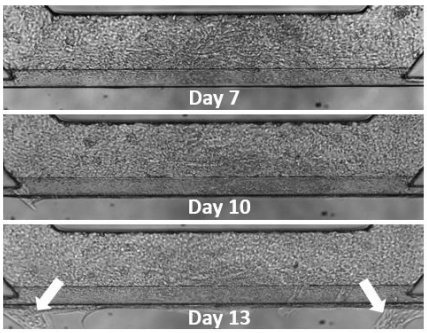

Supplementary figure S4: Stability of RPTEC tubules in the OrganoPlate. *RPTEC tubules are stable up to day 11. After this time period RPTEC start invading the ECM and the tubules are not leak tight anymore. Therefore, experiments should be performed during day 6 and day 11.*

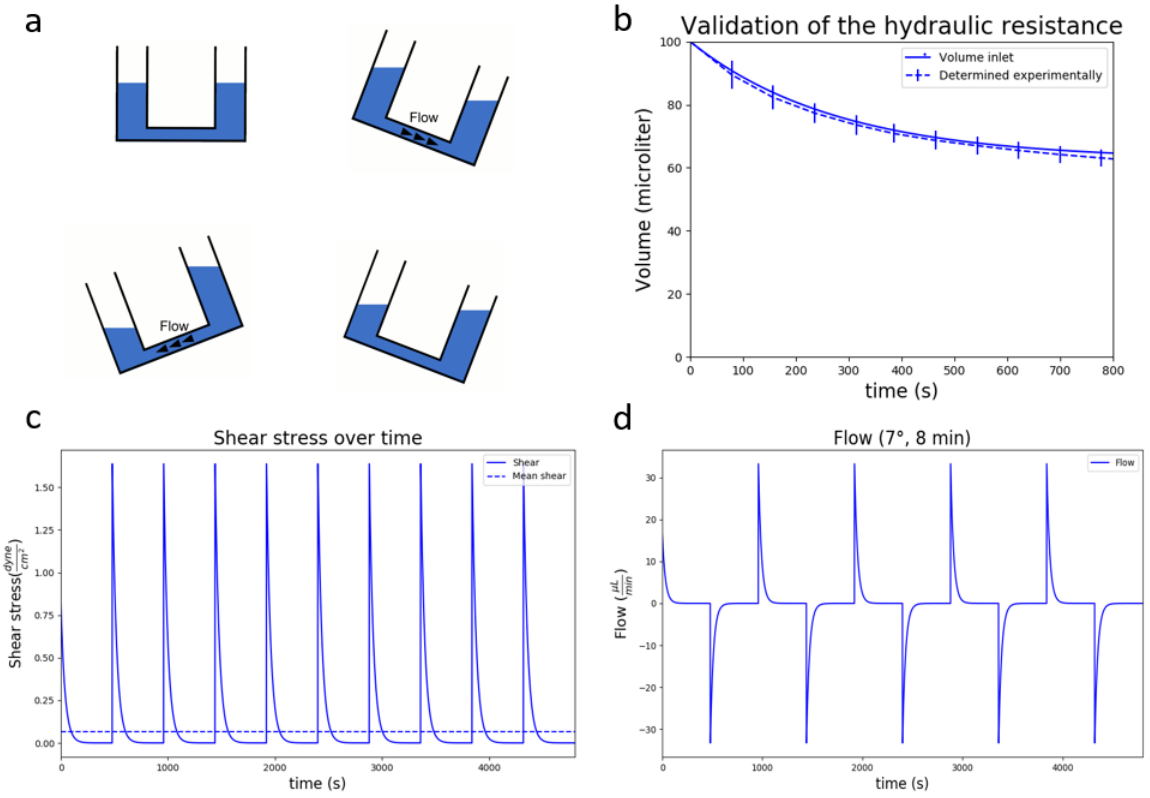

Supplementary figure S5: Validation of the hydraulic resistance. *a Schematic of how the flow is generated in the system. The OrganoPlate was placed in an incubator on an interval rocker platform (+/- 7 degree angle, 8 min interval) enabling a bidirectional flow though the perfusion channels. By placing one inlet to the microfluidic system higher than the other inlet gravity-based perfusion can take place. When the liquid levels in connected wells the plate is tilted and the liquid flows into the opposite direction. b Empirical validation of a numerical model of gravity drive flow in an OrganoPlate. Change in fluorescence due to flow of FITC solution between wells in a 9603200B OrganoPlate (2-lane plate with 120 x 200 µm, w x h channels) (Solid line) showed high correlation with the associated simulated volumes (dashed line). c Sheer stress in the microfluidic channel over time simulated for the 3-lane OrganoPlate with 400 µm wide channels. d Simulated flow rate over time calculated for the microfluidic channel of the 3-lane OrganoPlate with 400 µm wide channels.*

Supplementary Information

Flow rate and sheer stress

The platform described in this work uses a gravity-based perfusion system. When the liquid levels in connected wells are level, no difference in potential energy exists between the two wells, since the gravitational pull on the both volumes of fluid is identical, and no pressure difference exists between the two wells (fig. S5 a).

By periodically tilting a well plate with microfluidically connected wells, a height difference is imposed between the liquid levels in connected wells. The resulting pressure difference causes a fluid flow and associated shear stress.

The fluid flow rate and induced shear stress in the microfluidic channels of the OrganoPlate can be estimated using a numerical model simulated in Python (Python Software Foundation, USA). This model calculates the induced pressure difference between two volumes of fluid, which are present in two microtiter plate wells that are connected by a microfluidic channel. This pressure difference induces a fluid flow, with a flow rate that depends on the hydrodynamic resistance of the microfluidic channel and the fluid properties. This numerical model will be described in more detail below.

When a microfluidic chip is fully seeded, the inlet and outlet well of the perfusion channel are both filled with identical volume (50 µL). When the microtiter plate is levelled (0°) and both volumes are equal, an equilibrium is present: the gravity-induced pressure of both volumes of fluid is identical. The pressure, which is caused by the gravitational pull on a volume of fluid, is calculated by:

$$P = \frac{mg}{A} = \frac{\rho V g}{A} = \rho g h$$

In which pressure P (Pa) is calculated by dividing the weight of the fluid by the surface area of the microfluidic well. The weight is calculated by multiplying mass m (kg) with the gravitational constant g (9.81 m/s^2 or $N \cdot m^2/kg^2$). Since m can be calculated by multiplying volume V (m^3) with fluid density ρ (kg/m^3), the pressure is calculated by ρgh.

Now, the induced pressure of both volumes of fluid can be calculated. When the microtiter plate is tilted under a certain angle (e.g. 7°), the induced pressure of both volumes is different, resulting in a pressure difference. This difference results in the flow of fluid, whom flow rate can be calculated by:

$$Q = \frac{\Delta P}{R_h}$$

In which flow rate Q (m^3/s) is calculated by dividing the pressure difference ΔP (Pa) by the R_h ($kg/(m^4 \cdot s)$). This resistance is calculated by:

$$R_h = \frac{12\mu L}{wh^3(1 - 0.630h/w)}$$

In which w is the width (m) of the microfluidic channel, h the height of the channel (m), μ the fluid dynamic viscosity (0.001 kg/(m·s) or Pa·s), L the channel length (m) and R_h is the hydrodynamic resistance ($kg/(m^4 \cdot s)$)) of a channel with a rectangular cross-section (valid when h < w). This is validated by sequentially measuring the absorption at 494 nm of a 10 μg/ml Fluorescein in water (fig. S5 b). As the volume in the well changes over time, the absorption changes correspondingly. Now, this flow rate can be used to calculate the shear stress, which is exerted on the cells in the perfusion channel. This shear stress τ (Pa) is calculated by:

$$\tau[i] = \frac{6\mu Q[i]}{wh^2}$$

The flow of liquid from one well to the other reduces the difference in liquid level height and thus reduces pressure and flow rate. Numerical integration is used to approximate the flow and resulting shear stress and flow rate over time (fig. S5 c,d) for the settings used in this research.